ARTICLE NO. 79-1137R

Thrust and Ignition Transients of the Space Shuttle Solid Rocket Motor

Leonard H. Caveny*
Princeton University, Princeton, N. J.
Kenneth K. Kuo†
Pennsylvania State University, University Park, Pa.
Benjamin W. Shackelford‡
NASA Marshall Space Flight Center, Ala.

Techniques developed for predicting and analyzing ignition, pressurization, and thrust transients in large segmented motors were applied to the four developmental Space Shuttle solid rocket motors. Following the first test, attention was focused on understanding dynamic thrust and the rate of thrust increase during pressurization and predicting effects of reduced igniter mass flow rate and gas temperature. The close coupling between the igniter and the head-end segment and the high length-to-diameter ratio make understanding of the longitudinal pressure waves essential. The igniter performance along with igniter to head-end segment geometry govern the induction interval and head-end segment ignition. Following ignition of the head-end segment, subsequent flame spreading and pressurization tend to be motor properties which are not appreciably altered by changes in the head-end igniter mass flow rate.

Introduction

THIS paper reports on a project[1,2] directed at developing techniques for predicting and analyzing the ignition, pressurization, and thrust transients of the Space Shuttle solid rocket motor (SRM). Following the prediction and test of development motor number one (DM1), attention was given to understanding dynamic thrust and the rate of thrust increase during pressurization and predicting the effects of reduced igniter mass flow rate on the ignition transients.

Other studies have dealt with a specific process taking place during the start of solid propellant motors or have focused on practical correlations to facilitate igniter design. A detailed review of previous studies is given in Ref. 3. The analytical models directed at the analysis of the overall starting transient can be categorized into three major groups: 1) lumped chamber-parameter, or $p(t)$ models, which are used widely by the propulsion companies, 2) quasisteady one-dimensional flow, or $p(x)$ models, and 3) temporal and spatial development of the flowfield, the $p(x,t)$ model.[3] A $p(x,t)$ model which accounts for the interactions produced by the segments in the Space Shuttle SRM was developed as part of the project.

The $p(t)$ models assume uniform pressure and temperature distributions in the combustion chamber port. Accordingly, $p(t)$ models are incapable of considering those driving forces which control ignition and flame spreading rates along the port and interactions with the circumferential slots formed by the motor segments. In the $p(x)$ models, quasisteady pressure and velocity distributions along the port are assumed at each instant of time during the transient. Flame spreading calculations must be treated empirically and are thus unsuitable for predictive use.

Many high-performance solid propellant rocket motors have high volumetric loading densities, small port-to-throat area ratios, and frequently, large length-to-diameter ratios. Such motors are characterized by high internal gas velocities (e.g., maximum steady-state Mach numbers of 0.3 or higher), significant axial pressure and temperature gradients, pressure overshoots, and relatively short ignition transient times. The Space Shuttle SRM is in this classification and, thus, would be inadequately predicted and incompletely analyzed by either the $p(t)$ or the $p(x)$ models. In particular, pressure, temperature and velocity variations with time and axial position in the motor $p(x,t)$ model must be considered. Interactions between processes, such as the developing flowfield, flame spreading, and filling of the slots (between the segments) must be taken into account.

Analytical Approach

The ignition model begins with the onset of igniter flow and continues through the transient process to steady-state motor operation. The analytical techniques account for 1) the temporal and spatial development of the rocket motor internal flowfield set up by the igniter discharge, 2) first ignition, 3) flame spreading rates (along the several segments) coupled to main chamber and circumferential slot flows, 4) the large velocity, pressure, and temperature gradients that occur during the early phases of ignition, and 5) the interactions that combine to produce peak pressures, longitudinal waves and dynamic thrust components. The latter interactions include compression of chamber gases during pressurization, flow interactions with slots, mass-added effects of igniter discharge, and longitudinal waves impinging on the nozzle. The type of rocket motor configuration and events considered in the analysis are illustrated in Fig. 1.

The physical and mathematical formulation of the basic ignition model was given in Ref. 3. The extensions of the model to account for practical rocket motors and motors with circumferential slots are described in Ref. 1. The techniques

Presented as Paper 79-1137 at the AIAA/ASME/SAE 15th Joint Propulsion Conference, Las Vagas, Nev., June 18-20, 1979; submitted July 18, 1979; revision received April 11, 1980.

Index categories: Combustion Stability, Ignition, and Detonation; Solid and Hybrid Rocket Engines; LV/M Propulsion and Propellant Systems.

*Senior Professional Staff Member; presently, AFOSR/NA, Bolling AFB, D.C. 20332. Associate Fellow AIAA.

†Associate Professor. Member AIAA.

‡Aerospace Engineer, Propulsion Division.

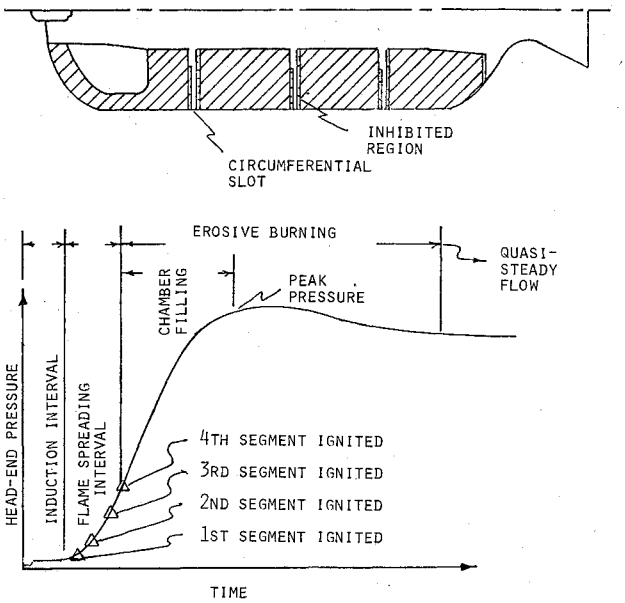

Fig. 1 Type of rocket motor configuration and time intervals considered.

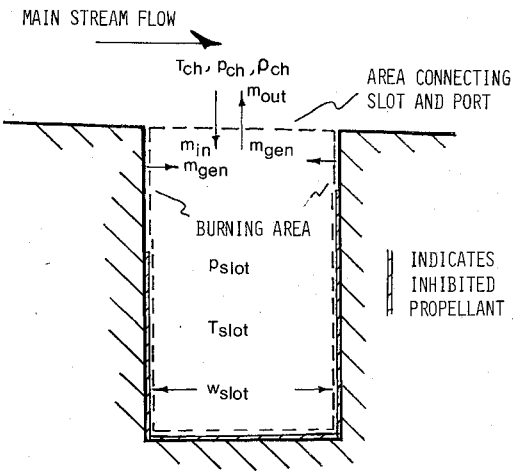

Fig. 2 Slot interactions considered in model.

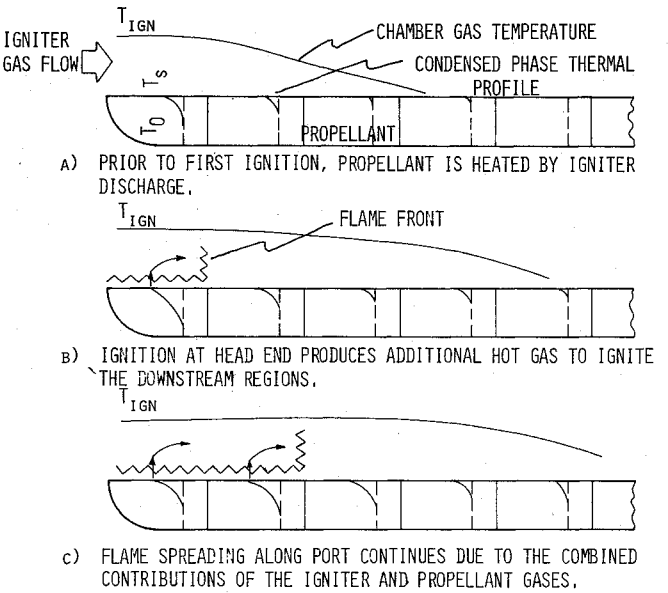

Fig. 3 Flame spreading along rocket motor port is a result of successive heatup-to-ignition of the axial increments.

for analyzing dynamic thrust are given in Ref. 2. Accordingly in this paper, only a phenomenological description of the model is given and the reader is referred to Refs. 1-3 for additional details and the mathematical formulation. The first application of the model to Space Shuttle size SRM's is described in Ref. 4. The mathematical formulations consist of the following: 1) mass, momentum, and energy conservation equations in unsteady, one-dimensional form for the gas phase; 2) equation of state for the gas flowing in the motor; 3) initial conditions at the start of the transient (onset of igniter flow); 4) two boundary conditions at the fore-end of the propellant section, obtained from a pair of ordinary differential equations, which describe the rate of change of pressure and temperature in the entrance section; 5) a third boundary condition, which describes the gas velocity at the entrance to the motor nozzle, for either choked or unchoked flow; 6) semiempirical correlations for the convective heat-transfer and friction coefficients for the highly turbulent flow in the port; 7) a burning rate law or table for the solid propellant, including the effects of initial temperature, pressure, and velocity over the surface (erosive burning); 8) a solid phase heatup equation for determination of the propellant surface temperature (at each axial increment) during the induction interval coupled to an ignition criterion for the propellant; 9) nozzle thrust equation based on nozzle end stagnation pressure; and 10) dynamic thrust based on rate of momentum change of chamber gases.

As shown in Fig. 1, segmented motors consist of a series of sections which when joined together form circumferential slots. In the case of the SRM, these slots contain an appreciable volume and a relatively small burning surface area. The interactions produced by the slots (see Fig. 2) are accounted for by solving a set of ordinary differential equations for each slot and using those solutions as boundary conditions for the main chamber flow equations (see Ref. 1 for details).

Flame spreading is governed by couplings between the main chamber flowfield, convective heating rates and the propellant temperature distribution. As illustrated in Fig. 3, the propellant area which is first exposed to the igniter discharge is heated at the highest rate. Flame spreading down the port is implicitly an output of the model, i.e.:

1) The hot gases from the igniter, as they flow down the port, heat the propellant.

2) The rate at which the propellant is heated rapidly decreases in the direction of flow because igniter gases give up their heat as they flow toward the nozzle.

3) After the head end of the motor ignites, the flow rate of hot combustion gases along the port begins to accelerate and thereby accelerates the heating of the preheated (but unignited) propellant.

4) As the flow rate increases, the acceleration of the combustion gases becomes one of the limiting factors and flame spreading rate becomes largely a characteristic of the motor and not the igniter.

5) As the hot combustion gases are driven down the port, the propellant is progressively heated to its ignition point, which is to say that flame spreading is described by successive ignitions.

The intrinsic capability of the $p(x,t)$ model to calculate flame spreading rates is one of its main features.

In the Space Shuttle SRM, the nozzle of the head-end igniter is relatively close to the star-point tips in the first motor segment. Treating the head-end region as a uniformly heated port results in an unrealistically long induction period. A good simulation is obtained by considering three zones of heating and ignition in the first motor segment: 1) the more intense heating and rapid ignition of the star-point tips, 2) the increasing heating rate in the axial slots as the gases generated by the burning star-point tips augment the axial flow of igniter gases, and 3) the conventional heating of the aft portion of the first motor segment.

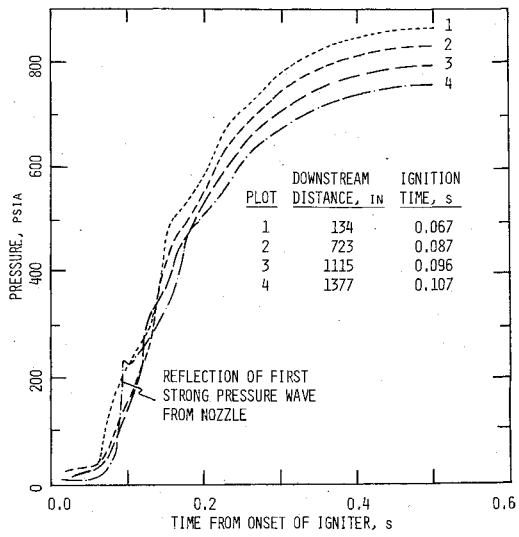

Fig. 4 Pressure development along port of segmented motor.

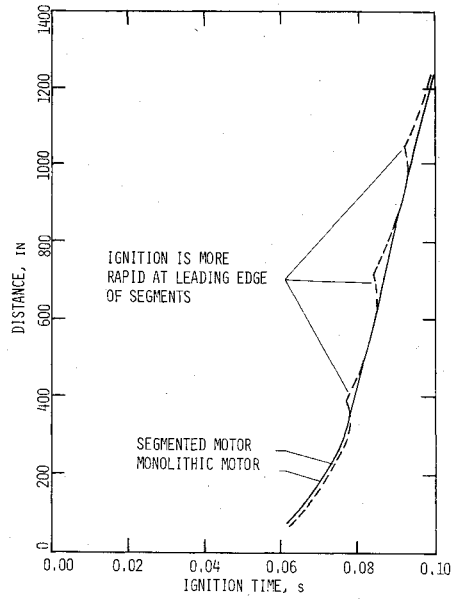

Fig. 5 Flame spreading times of segmented motor compared to flame spreading times of comparable monolithic motor.

Figure 4 shows the calculated pressure vs time at four positions along the port. It shows the reflection of the first strong wave (arriving at the nozzle) and subsequent longitudinal pressure oscillations as the chamber filling continues.

Once the first motor segment ignites, the subsequent flame spreading rate (along the downstream motor segments) is essentially a motor property that is largely unaffected by changes in the igniter characteristics, whereas the time of first ignition is strongly dependent on igniter characteristics and the propellant ignition properties. Figure 5 shows the flame spreading position as a function of time. The flame spreading process in the downstream segments proceeds at a nearly constant rate. The energy required to accelerate the gases down the chamber has the effect of limiting the velocity of the axial waves and, hence, the flame spreading rate. The higher heat transfer rates at the leading edge of each segment produce somewhat higher flame spreading rates near the leading edge of each segment (see Fig. 5). The contributions of the burning surface areas and volumes in the circumferential slots of the present SRM design do not greatly influence the times of the important ignition events. However, the interactions of the main chamber flow with the circumferential slots tend to damp axial pressure waves which are set up toward the end of flame spreading. The net effect of the close coupling between the igniter and the star-point tips is to reduce the induction time which is a major contributor to the uncertainty associated with motor-to-motor variation in time to liftoff thrust.

Included in Fig. 5 are results for a monolithic motor with equivalent burning surface area and length. These results illustrate that the overall flame spreading rate is not greatly affected by the slots.

Dynamic and Static Thrust

In this analysis a distinction is made between static thrust and dynamic thrust. Static thrust is the widely used conventional concept of thrust produced by gases flowing through a rocket motor nozzle. Dynamic thrust is that component of total thrust which is produced by such events as rapidly accelerating changes in the internal rocket motor flowfield, rapid relative movement of the propellant or inert hardware, sudden changes in flow area (e.g., nozzle removal or vent port opening), and ejection of objects through the nozzle. Those concepts are developed more fully in Ref. 2. Dynamic thrust is seldom of interest in the applications of conventional rocket boosters and sustainers. However, the Space Shuttle SRM is sufficiently long, 125 ft (~39 m), that the dynamic thrust events associated with establishing the flowfield are significant. Indeed, the thrust vs time records of the first static test of the Space Shuttle SRM (DM1) reveal transient forces on the order of 1.3 MN (300,000 lbf) during the first 100 ms of motor operation. Figure 6 is a plot of the measured thrust vs time record for DM1 and several prominent events are indicated. Coinciding with what is calculated to be the onset of flame spreading is a rapid increase in thrust. The thrust between 0.02 and 0.08 s occurs before flow through the nozzle is established and, thus, is attributed to the momentum changes of the gases flowing within the chamber. The periodic disturbances as thrust increases are attributed to the longitudinal wave action within the chamber and to oscillations of the propellant and case masses.

Figure 7 shows pressure rise and thrust events during the induction, flame spreading, and initial pressurization phases. The dynamic thrust contribution is prominent during the time of flame spreading and decays rapidly as the longitudinal pressure wave encounters the aft-end of the motor. The nonuniform thrust rise rates correspond to the longitudinal pressure waves interacting with the nozzle. The parametric calculations reveal that the time relationship between the igniter flow arriving at the nozzle and the surge of hot gases from the head-end segment affects the magnitude of the thrust rise rates. If the igniter gases lead (by a sufficient period) the gases from the head-end segment, both the dynamic thrust contribution is diminished and the effects of strong longitudinal pressure waves are attenuated.

Comparison With Motor Data

As described in Ref. 5, several ignition transient requirements are imposed on the SRM. The motor must reach 1.9 million pounds thrust within the time period of 0.15-0.45 s (i.e., the ignition interval) and the maximum rise of thrust should not exceed 150,000 lbf within any 10 ms period. The ignition interval requirement was met easily. However, the maximum thrust rise rate for DM1 was 355,000 lbf over 10 ms (see Fig. 6).

The preparations for the test of DM2 included the consideration of methods of reducing thrust rise rate. Two changes in the igniter were considered during the parametric studies: reducing the flame temperature and reducing mass flow rate. Figure 8 shows the igniter mass flow rates corresponding to each test. The two sets of lines on Figs. 9 and 10 correspond to the mass flow rates of the DM1 igniter

and the mass flow rate of the DM2 igniter (which is 73% of the DM1 mass flow rate). The calculated results reveal that the igniter propellant flame temperature could be decreased by 400 K and the ignition interval requirement would still be satisfied (Fig. 9), but that the decrease in thrust rise rate would not be sufficient (Fig. 10). Calculations for the DM3 conditions (i.e., 49% decrease in mass flow rate) also indicated that significant decreases in thrust rise rates would not occur.

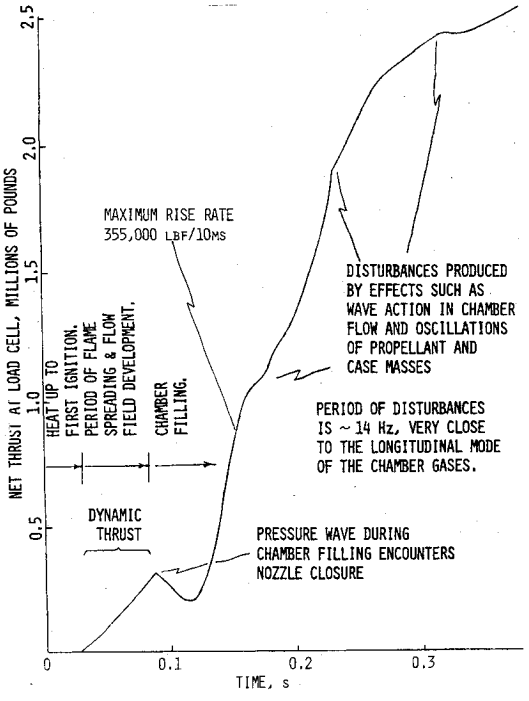

Fig. 6 Thrust transients noted on plot of measured net thrust vs time for the first static test of the Space Shuttle solid rocket motor (DM1).

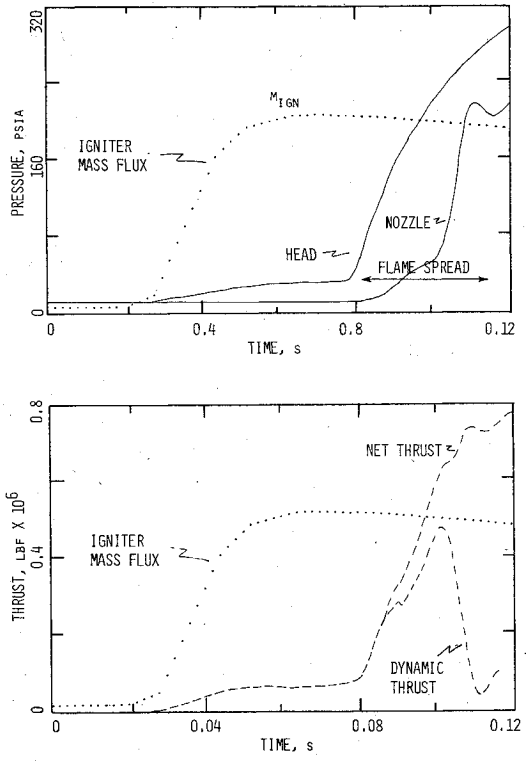

Fig. 7 Dynamic thrust builds up as pressure wave travels down grain and decays as pressure wave encounters nozzle.

An examination of measured and calculated head-end pressures (Fig. 11), reveals an increase in ignition time corresponding to the reduction in igniter mass flow rate. However, the overall pressurization rates and effects of longitudinal wave action are affected only moderately. The measured and calculated thrusts (Fig. 12) show that reducing the igniter mass flow rate reduces the dynamic thrust but that

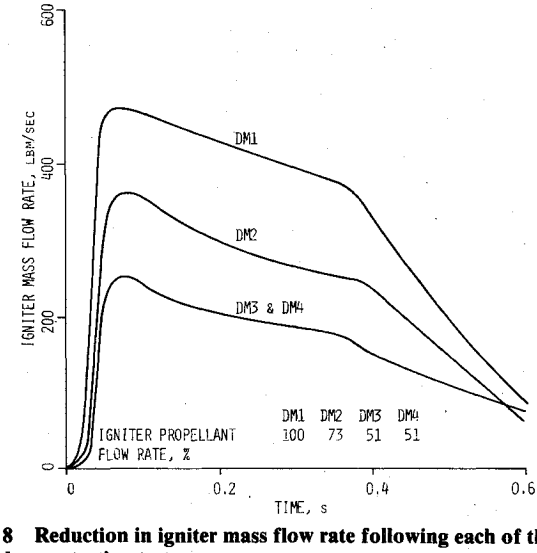

Fig. 8 Reduction in igniter mass flow rate following each of the first two demonstration tests.

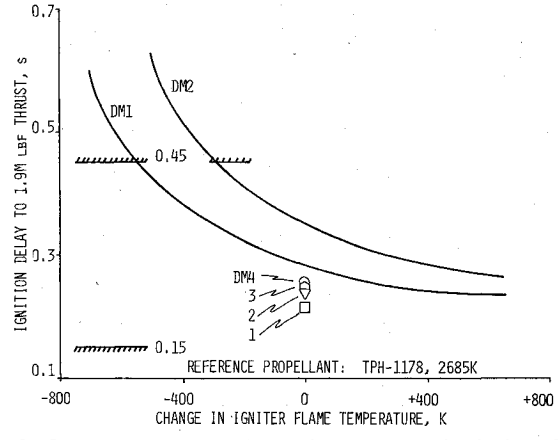

Fig. 9 Increased ignition time with decrease in igniter flame temperature and mass flow rates (DM2 igniter flow rate was 73% of that of DM1).

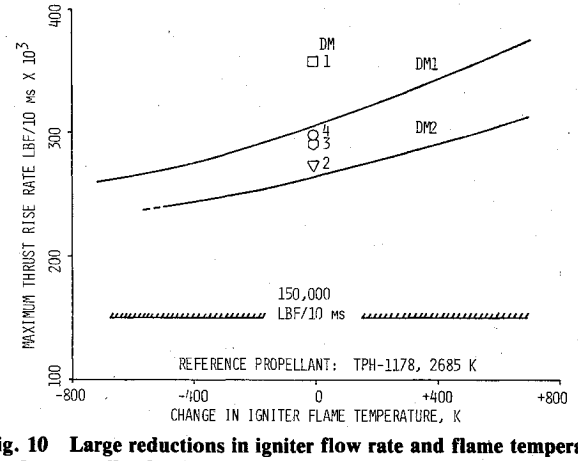

Fig. 10 Large reductions in igniter flow rate and flame temperature produces small reductions in maximum thrust rise rate.

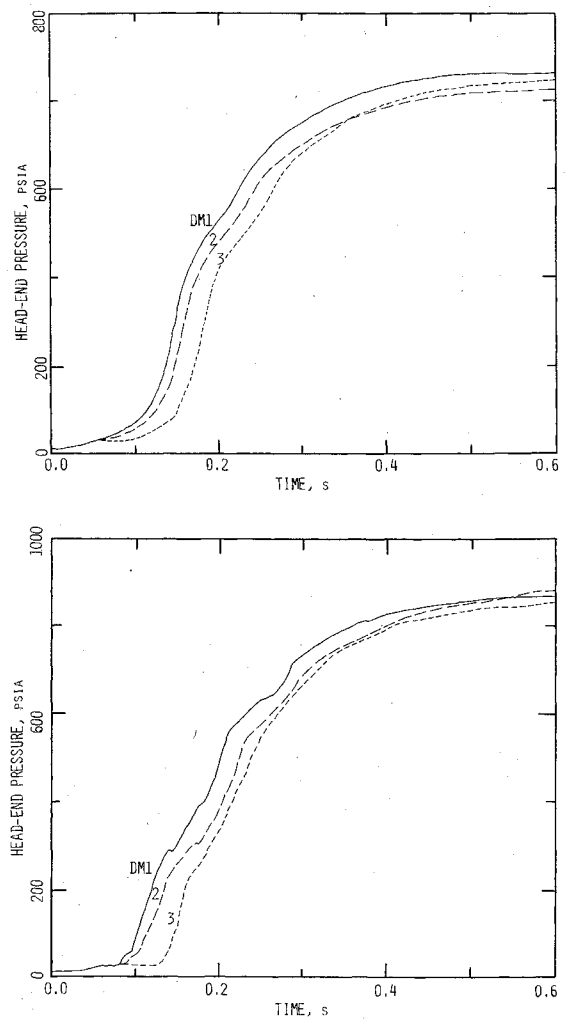

Fig. 11 Measured (top) and calculated (bottom) head-end pressures corresponding to changes in igniter mass flow rate.

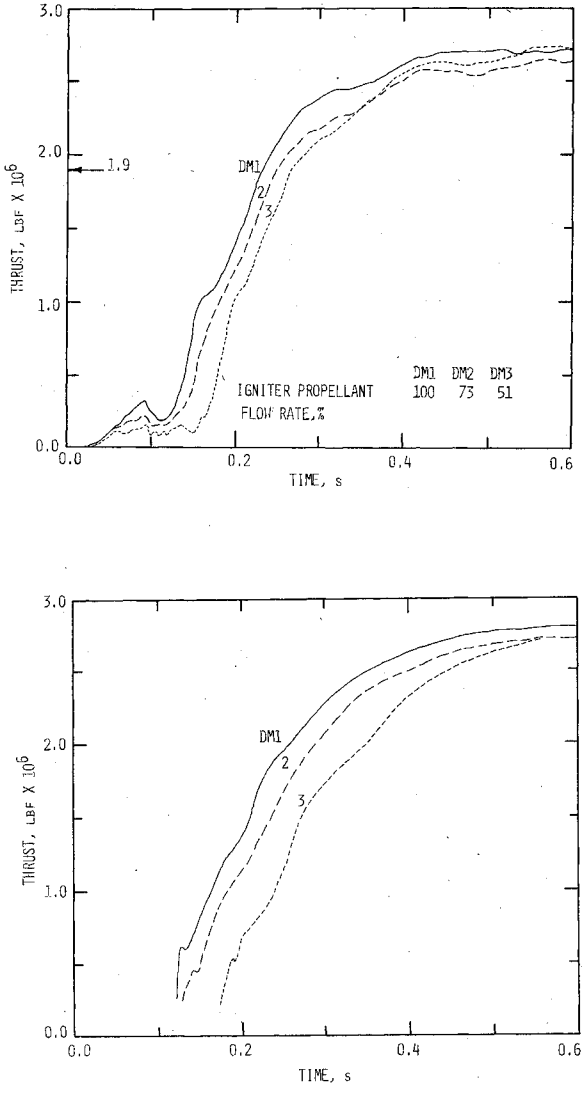

Fig. 12 Measured (top) and calculated (bottom) thrusts showing that decreasing igniter output delayed onset of rapid thrust rise but did not diminish oscillations that produced undesirably high thrust rise rates.

the increases in thrust rise rates associated with the longitudinal wave action have the same character and magnitude.

The dynamic thrust component and the increase in thrust corresponding to the longitudinal pressure waves arriving at the nozzle have the proper trends with respect to the measured thrust. However, the measured net thrust is a result of fluid flow dynamics as well as the dynamics of motor case axial expansion and axial movement of the large propellant masses. Thus, the calculations in this paper do not include all of the elements required to determine net thrust and to correct for thrust stand errors. Additional aspects of these processes are considered in Ref. 6. It should be kept in mind that the contributions to thrust dynamics associated with hardware movement will be different under vertical launch conditions than under the horizontal static test conditions.

A comparison of the calculated and measured results of Figs. 11 and 12 reveals that the important trends are accounted for. The physical situation is sufficiently complex that the magnitude of time intervals and thrust oscillations cannot be calculated precisely.

Conclusion

The analytical model described in this paper provides for the first time a means of analyzing the complexities of ignition transients and pressure peaks of large, high-performance, segmented rocket motors. This is accomplished by accounting for 1) the temporal and spatial development of the flow field set up by the igniter discharge, 2) ignition and flame spreading coupled to chamber flow, 3) the large velocity, pressure, and temperature gradients that occur during the early phases of ignition, and 4) the interactions that combine to produce peak pressures (i.e., compression of chamber gases during pressurization, erosive burning, and mass-added effect of igniter discharge).

Once the head-end section of the SRM ignites, the subsequent flame spreading rate is a motor property that is largely unaffected by changes in the igniter and by propellant variation, whereas the time of first ignition is strongly dependent on igniter characteristics and propellant ignition characteristics. The contributions of the burning surface areas and volumes in the circumferential slots of the present SRM design do not greatly influence the times of the important ignition events.

As the pursuit of higher performance rocket motors continues and the present configurations are upgraded (i.e., by increasing loading density, using high-performance propellant, and extending ambient temperature range), the methods described in this paper and in Refs. 1-3 will enable analysts to predict items such as ignition delays, rate of thrust increase, maximum pressures, and igniter flow rates with much greater confidence than was heretofore possible. The ignition prediction and analysis procedures described in the paper can be applied to a wide variety of rocket motors and are not limited to large segmented boosters.

Acknowledgments

This project was supported by the NASA Marshall Space Flight Center. The project applied and extended analytical techniques which originated with a series of grants to Princeton University administered by NASA Langley and the Jet Propulsion Laboratory. Accordingly, it incorporates some of the results the authors obtained in a previous collaboration with A. Peretz and M. Summerfield.

References

[1] Caveny, L. H. and Kuo, K. K., "Ignition Transients of Large Segmented Rocket Boosters," NASA Contractor Report CR-150162, April 1976.

[2] Caveny, L. H., "Extensions to Analysis of Ignition Transients of Segment Rocket Motors," NASA CR-150632, Jan. 1978.

[3] Peretz, A., Caveny, L. H., Kuo, K. K., and Summerfield, M., "The Starting Transient of Solid-Propellant Rocket Motors With High Internal Gas Velocities," AMS Report No. 1100 and NASA CR-136274, Princeton University, Princeton, N. J., April 1973 (Order from NTIS as N 74-13506); also summarized in *AIAA Journal*, Vol. 11, Dec. 1973, pp. 1719-1727.

[4] Caveny, L. H., Peretz, A., and Summerfield, M., "Thrust Transients of Large Solid Rocket Motors," *Proceedings of 10th JANNAF Combustion Meeting*, Vol. I, CPIA Publ. 243, Dec. 1973, pp. 21-44.

[5] Adams, I. C. and Call, F. W., "Space Shuttle SRM Development," *Proceedings of 1979 JANNAF Propulsion Conference*, April 1979.

[6] Mason, D. R., Folkman, S. L., and Behring, M. A., "Thrust Oscillations of the Space Shuttle Solid Rocket Booster Motor During Static Tests," AIAA Paper 79-1138, June 1979.